SEMARAK ILMU PUBLISHING
202103268166(003316878-P)

Journal of Advanced Research in Applied Mechanics

Journal homepage:
https://semarakilmu.com.my/journals/index.php/appl_mech/index
ISSN: 2289-7895

The Influence of Topology Optimisation and Material Stiffness of Dental Implant on Fatigue Behaviours – A Finite Element Analysis

Muhammad Ikman Ishak[1,*], Ruslizam Daud[1], Siti Noor Fazliah Mohd Noor[2], Khor Chu Yee[1], Husniyati Roslan[2]

[1] Fakulti Kejuruteraan & Teknologi Mekanikal, Universiti Malaysia Perlis (UniMAP), Kampus Alam UniMAP, Pauh Putra, 02600 Arau, Perlis, Malaysia
[2] Advanced Medical and Dental Institute, Universiti Sains Malaysia, Bertam, Jln. Tun Hamdan Sheikh Tahir, 13200 Kepala Batas, Pulau Pinang, Malaysia

ARTICLE INFO

Article history:
Received 25 October 2023
Received in revised form 27 December 2023
Accepted 13 January 2024
Available online 23 February 2024

Keywords:
Dental implant; fatigue; finite element analysis; material stiffness; topology optimisation

ABSTRACT

The resilience of a dental implant in restoring occlusion relies on biomechanical stress factors, including implant macrostructures, parafunctional oral behaviours, and the choice of materials. Topology optimisation stands out as a leading approach for enhancing system performance. Different implant designs and materials may have divergent impacts on load distribution at the bone-implant interface. There exists a shortage of published information addressing topologically optimised dental implants and the impact of implant material stiffness, creating a persisting ambiguity on the topic. The novelty of the study lies in the determination of excess material distribution within a dental implant and the influence of different implant stiffnesses through computational fatigue analysis. This study aimed to evaluate the fatigue characteristics of regular and topologically optimised dental implant configurations across various implant materials, employing three-dimensional finite element analysis. Geometric models were developed following ISO 14801 standards using SolidWorks 2020, and subsequently, analysed in ANSYS 18.1. Each implant design (regular, optimised design 1, and optimised design 2) was subjected to three different material stiffnesses indicated by cpTi, Ti-6Al-4V, and zirconia. The model was exerted by a 200-N inclined load. Compared to the regular implant, the topologically optimised implants exhibited a decrease in implant stress ranging from approximately 3.4% to 11.9%. However, the regular design yielded a longer fatigue life, surpassing that of the optimised designs by about 33.8% to 75.9%. Concerning safety factors, the optimised implants displayed safety factor levels that were nearly 3.5% to 13.5% greater than those of the regular implant. Among all the materials, the implant with higher stiffness was found to be advantageous, as it resulted in reduced implant stress, extended fatigue life, and increased safety factor compared to the less stiff implant, regardless of the implant designs.

* *Corresponding author.*
E-mail address: ikman@unimap.edu.my

https://doi.org/10.37934/aram.114.1.109124

1. Introduction

Endosteal dental implants stand out as a common preference for addressing the dental needs of both completely and partially edentulous patients, serving to rehabilitate oral functionality and enhance aesthetic appeal [1, 2]. These surgically implanted devices are consistently in high demand and have demonstrated a track record of success and longevity that is regarded as satisfactory [3, 4]. Titanium, recognised for its biocompatible properties, takes the lead as the most commonly employed material for dental implants, contributing significantly to the implant stability and overall effectiveness. Within the realm of endosteal dental implants, the root form implant occupies a prominent position, as it encompasses the vertical bone region, closely replicating the structural characteristics of a natural tooth root [5]. Root form implants come in diverse configurations, with the cylindrical and screw-type variations emerging as the most prevalent. These design options can be found in both solid and hollow forms. The introduction of hollow-cylindrical implants aims to augment the total contact surface area between the implant and the surrounding bone tissue when compared to their solid-cylindrical counterparts. The solid-cylindrical implant design faces potential challenges associated with shear forces and frequently relies on surface treatments to enhance its integration with the adjacent bone structure. In contrast, solid-screw implants are characterised by macroscopic retention features along their surfaces, facilitating primary anchorage within the bone tissue. Beyond mitigating shear forces, these retentive elements may also serve to reduce the risk of overloading at the interface between the implant and the adjacent bone. Solid-screw implants present enhanced functional contact surfaces with the surrounding bone and facilitate simplified surgical implantation, particularly when compared to hollow-screw or hollow-cylindrical shapes.

Endosteal dental implants stand out as a common preference for addressing the dental needs of both completely and partially edentulous patients, serving to rehabilitate oral functionality and enhance aesthetic appeal [1, 2]. These surgically implanted devices are consistently in high demand and have demonstrated a track record of success and longevity that is regarded as satisfactory [3, 4]. Titanium, recognised for its biocompatible properties, takes the lead as the most commonly employed material for dental implants, contributing significantly to the implant stability and overall effectiveness. Within the realm of endosteal dental implants, the root form implant occupies a prominent position, as it encompasses the vertical bone region, closely replicating the structural characteristics of a natural tooth root [5]. Root form implants come in diverse configurations, with the cylindrical and screw-type variations emerging as the most prevalent. These design options can be found in both solid and hollow forms. The introduction of hollow-cylindrical implants aims to augment the total contact surface area between the implant and the surrounding bone tissue when compared to their solid-cylindrical counterparts. The solid-cylindrical implant design faces potential challenges associated with shear forces and frequently relies on surface treatments to enhance its integration with the adjacent bone structure. In contrast, solid-screw implants are characterised by macroscopic retention features along their surfaces, facilitating primary anchorage within the bone tissue. Beyond mitigating shear forces, these retentive elements may also serve to reduce the risk of overloading at the interface between the implant and the adjacent bone. Solid-screw implants present enhanced functional contact surfaces with the surrounding bone and facilitate simplified surgical implantation, particularly when compared to hollow-screw or hollow-cylindrical shapes.

Various factors influence the biomechanical compatibility of dental implants, encompassing parameters like implant geometry, occlusal loads, material stiffness of the implant body, implant dimensions, and the quantity and quality of implanted bone [6, 7]. The attachment between the implant and the adjacent living tissues is characterised by the phenomenon of osseointegration. In the initial stages of implantation, it is common to observe marginal bone loss due to reduced mechanical triggers. Elevated stress levels and localised concentration, particularly around the implant neck, may signal the potential for bone loss [8]. In cases of low-quality bone, the preference tends to lean toward implants with larger diameter and longer, straight body walls. Additionally, implementing the concept of platform switching in dental implants, wherein the abutment diameter is notably smaller than the implant platform, leads to decreased compressive and tensile bone stresses when contrasted with implants that have matching platforms [9]. Platform-switched implants contribute to the preservation of alveolar bone levels by redistributing stresses from the cortical bone region to the cancellous bone region. When it comes to applied loads and bone quality, these two variables pose challenges in achieving an optimal stress level at the bone-implant interface. Numerous endeavours have been undertaken to enhance the design of dental implants, with attempts to mimic the natural tooth shape. Optimised implant designs featuring tapered and broader necks have demonstrated substantially lower peak stress levels when compared to regular implant designs [10].

Topology optimisation is a technique utilised to allocate materials efficiently within a given design space, adhering to specific loads and constraints [1, 11, 12]. Essentially, it is a method for optimising the shape of structures to determine material distribution. An optimal structural configuration aims for uniform stress distribution within the body, limited to acceptable levels. It is feasible to remove material from regions with minimal stress, allowing the final design to maintain its function with decreased mass. For example, a topologically optimised spinal cage design successfully decreased the volume of the existing structure by around 36%, simultaneously creating more area for bone grafting while preserving spinal stability [13]. Besides, Nayak *et al.,* employed the topology optimization technique to identify potential structural designs for minimizing mass and enhancing the performance of the transtibial prosthesis socket. The proposed method involves the redesign of the socket, aiming to improve patient comfort through a customised design [14]. In a different study conducted by Khan *et al.,* the investigation's findings indicated the feasibility of achieving weight reduction in a mono leaf spring. This reduction aims to create a lightweight yet structurally robust design suitable for application in electric vehicles [15]. Concerning dental implants, elevated stresses are typically noticed at areas where they interface with the high-density bone, while low-value stress tends to build up at the apical region of implant. The essence of topology optimisation lies in its utilisation of mathematical algorithms, which center on objective functions, design factors, and supports [16]. By employing finite element analysis (FEA), the iterative optimisation procedure assesses the design's performance, systematically removing unnecessary materials while preserving structural integrity and functionality. FEA stands as a highly esteemed and universally embraced approach for tackling intricate mathematical challenges linked to stability and failure analysis in a multitude of domains, such as structural engineering, electronics, biomedicine, heat transfer, and fluid dynamics [17, 18]. Implant dentistry first witnessed the use of FEA as far back as 1973, and it has since seen growing adoption in forecasting outcomes that prove elusive in both experimental and clinical investigations. Until now, there is a scarcity of published information available concerning topologically optimised solid dental implants, leaving this issue shrouded in uncertainty and lacking a definitive conclusion. Chang *et al.,* conducted a study in which they noted a potential reduction of approximately 17.9% in the volume of the initial implant design [11]. The research examined an implant positioned within the maxillary first molar area and subjected it to a static occlusal force. Besides, Gupta *et al.,* conducted a more recent study, revealing that the implant could achieve a volume reduction ranging from 32% to 45%, all while maintaining its functional capabilities [1]. Under the consistent application of a static load, the study examined differences in implant length and diameter, as well as bone quality. Repetitive occlusal loading poses a significant risk of fatigue failure for dental implants. In previous computational research, the focus has predominantly been on assessing the performance of standard implants and analysing the ideal implant structure under static loading conditions, with less attention placed on investigating fatigue attributes. A comprehensive understanding of fatigue conditions is vital for gaining insight into how forces are transmitted within a dental implant assembly.

The material used in the production of dental implants must meet the physical, biological, and mechanical requirements, as these implants are directly interfaced with living tissues and endure significant occlusal forces. To mitigate the stress shielding effect, the implant material is designed to possess properties that closely resemble those of bone, thereby preventing excessive bone stress adaptation. Ceramics and titanium represent typical material choices for the construction of dental implants. Among commercially pure titanium (cpTi) grades, grade IV stands out for its superior strength, which explains its widespread adoption in the market. Furthermore, the titanium alloy known as Ti-6Al-4V, falling under grade V, boasts enhanced fatigue resistance and yield strength, solidifying its status as one of the leading material choices. On the contrary, ceramics like zirconia offer a more aesthetically pleasing alternative to titanium, meeting patients' demands and expectations. The subject of how various materials affect implant stability continues to be a matter of discussion and lacks clear consensus. There is a scarcity of information regarding the optimal selection of implant materials, highlighting the need to prioritize implant design before fabrication.

In this study, the primary aim was to investigate and draw comparisons of fatigue behaviours between the regular and topologically optimised dental implant configurations when subjected to varying material stiffnesses or types, utilising three-dimensional (3-D) FEA. Four distinct result criteria were extracted, which encompassed the following: the highest equivalent alternating stress, the shortest fatigue life, and the lowest safety factor. The null hypothesis posited that there would be no significant difference in the response data under investigation between the conventional and topologically optimised implant designs for different implant materials. Our study introduced a unique perspective by focusing on uncovering the distribution of excess material within a threaded dental implant. Additionally, it aimed to produce more precise quantitative data regarding fatigue responses for regular and topologically optimised designs by varying material stiffness. The findings could offer valuable guidance to clinicians and/or implant manufacturers looking to create novel implant macrogeometry designs that feature reduced mass while maintaining sufficient strength. Moreover, it is envisioned that this study will contribute to a better grasp of how force is transferred within diverse implant designs and materials when assessing their response to fatigue conditions.

2. Materials and Methods

2.1 Development of Experimental and Implant Part Models

The commercial dental implant system known as Dual-Fit (DFI) served as the reference for constructing a 3-D model of a solid threaded dental implant, produced by Alpha-Bio Tec, Petach Tikva. This implant has dimensions of 3.75 mm in diameter and 11.5 mm in length for its implant body. Additionally, the model included a straight abutment with a height of 3.5 mm, along with an abutment screw measuring 2.2 mm in width and 8.0 mm in length, which serves to securely place the abutment on the implant body. In the present study, the implant platform was configured with an internal hexagonal connection, aligning with the specifications detailed in the manufacturer's catalogue. Beyond the implant components, the 3-D geometrical modelling also encompassed a holder sized at 40.9 mm in length, 39.8 mm in height, and 23.0 mm in width, a hemispherical cap measuring 6.5 mm in length and 5.1 mm in width, as well as a loading structure with dimensions of 12.0 mm in length and 11.0 mm in width. Given the focus of the study on fatigue prediction, the 3-D model setup adhered to the standards outlined in the fatigue testing standard ISO 14801. This setup was created using computer-aided design (CAD) software, specifically SolidWorks 2020 from SolidWorks Corp. in Concord, Massachusetts, USA. The models were designed using a range of inherent geometric shape creation tools available in the software, including revolve, mirror, extrude, loft, sweep, and revolve.

Under the parameters outlined in ISO 14801, the parts were combined to create an assembly and subjected to testing conditions. In Figure 1(a), it shows an assembly model of the final setup configuration model. To position the implant body within the holder, a virtual embedding process took place within a 4.5-mm diameter cylindrical cavity created in the holder. This was achieved using the Boolean subtraction option. For simulation purposes, a 3.0-mm bone loss, determined from the holder surface to the implant platform as depicted in Figure 1(b), was incorporated. Subsequently, the abutment and its accompanying screw were affixed to the implant body. The hemispherical cap was then carefully placed on top of the abutment to facilitate loading. A critical alignment step ensured that the central axes of the implant body, abutment, screw, and cap all converged harmoniously. To represent a moment arm accurately, the central point of the cap was established at a distance of 11.0 mm from the bone (holder) level. Subsequently, the assembly model was exported into ANSYS 18.1 software from ANSYS Inc. (Houston, TX, USA). In this software, the model mesh was generated, and pre-processing settings for computational analysis were configured.

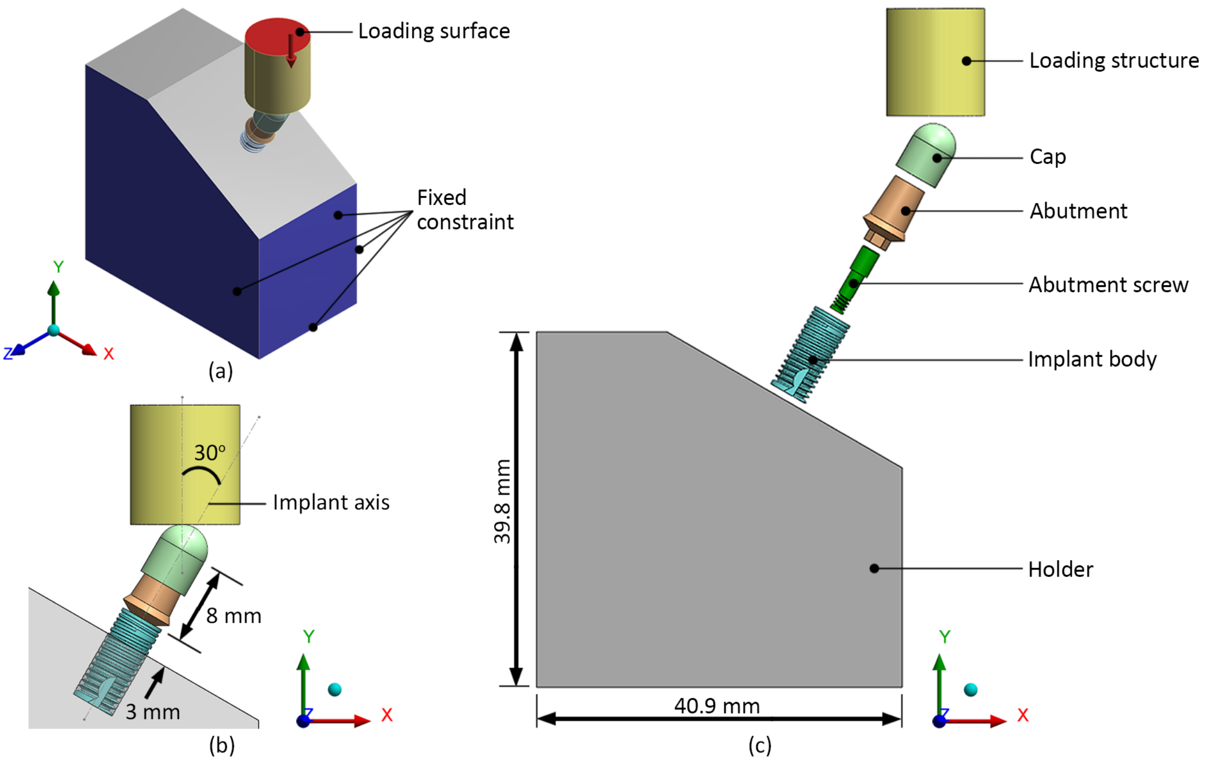

Fig. 1. (a) Assembly view of the model showing the loading and support locations (b) Specifications for implant positioning (c) Exploded representation of each part model

2.2 Pre-processing of Finite Element Analysis

In the model, each individual component was deemed to possess properties of isotropy, homogeneity, and linear elasticity. The abutment screw and abutment were all made of titanium alloy (specifically, Ti-6Al-4V) with a yield strength of 847 MPa [19]. For the implant body, it was analysed in three different implant material stiffnesses which are Ti-6Al-4V, commercially pure titanium (cpTi), and zirconia. These materials are widely recognised as the primary options for constructing the implant body. In contrast, the hemispherical cap and loading structure were constructed from a steel alloy. Adhering to the stringent criteria outlined by ISO 14801, it was necessary to ensure that the implant body was firmly secured within a clamping holder possessing an elastic modulus of at least 3.0 GPa. Consequently, for the purpose of this study, we selected aluminium alloy as the material of choice for the holder. A summarised overview of the material properties applied in configuring the model setup is available in Table 1.

Table 1
The properties of the materials in the model configuration

Material	Component	Modulus of Elasticity, *E* (MPa)	Poisson's Ratio, *v*	References
Steel alloy	Loading structure and cap	200,000	0.31	Yao *et al.,* [20]
Aluminium alloy	Holder	71,000	0.33	Bayata *et al.,* [21]
Ti-6Al-4V	Implant body, abutment, and abutment screw	113,800	0.342	Yalçın *et al.,* [22]
cpTi	Implant body	110,000	0.35	Brune *et al.,* [23]
Zirconia	Implant body	200,000	0.3	Tretto *et al.,* [24]

In ANSYS software, we created model interfaces with perfect bonding, employing both contact and target elements. Numerous earlier research works have also adopted this approach for simulating contact interactions [25]. The bonded contact classification ensures that there is no occurrence of penetration or slackening within the various interfaces, including those between the implant body-holder, abutment screw-implant body, abutment-abutment screw, abutment-implant body, cap-abutment, and cap-loading structure.

Following ISO 14801 guidelines for replicating the experimental testing conditions, we exerted a vertical force onto the flat surface of the loading structure model. This force setup effectively mimics an inclined load, positioned at a 30° angle relative to the implant's central axis [26]. The compressive load of 200 N was applied, representing normal biting force [27]. The load was positioned 11.0 mm away from the inclined surface of the holder.

In order to foresee how the implant system assembly would respond mechanically and exhibit fatigue behaviours, a fatigue analysis was conducted. This analysis utilised ANSYS software and involved simulating sets of masticatory loading sequences, as previously described. The fatigue algorithm employed was based on the Goodman fatigue theory within the elasticity mode. The analysis not only predicted fatigue lifespans but also identified regions at risk of potential failures according to the infinite fatigue life criteria.

Concerning the model's boundary conditions, constraints were imposed on all nodes located along the vertical and lower surfaces of the holder, restricting movement in all degrees of freedom. This dictates that the nodal displacement along these surfaces remains fixed. The loading and support locations assigned in the analysis are illustrated in Figure 1(a).

2.3 Configuration of Topology Optimisation

In clinical settings, the prevailing approach in dental implant design involves employing a circular cross-sectional configuration. This particular design exhibits limited resistance to shear and torsional forces, especially during the tightening of the abutment screw or when the implant stands independently. To enhance the potential for bone ingrowth without compromising structural integrity, anti-rotational features like vents or apical holes have been considered for inclusion in the implant body. In the pursuit of innovating a dental implant design that prioritizes the enhancement of the implant body's internal contact surfaces, the topology optimisation tool offered by ANSYS software was employed. It is crucial to emphasise that while decreasing the volume, the implant body's strength must be preserved.

Topology optimization primarily aims to diminish the energy related to structural compliance. Achieving a reduction in compliance equates to fortifying the overall stiffness of the structure. The standard approach to this method involves minimizing structural compliance while concurrently adhering to constraints on structural volume.

The density variable, denoted as η, spans from 0 to 1. A value approaching 1 signifies the necessity to retain the material, whereas a value approaching 0 implies the material should be eliminated. In the optimisation analysis, the goal was to reduce the volume of the entire regular implant body, or design domain, by approximately 50%, employing 10 iterations based on predefined response constraints. The convergence accuracy criterion was set at 0.1%. To achieve this, a 100-N vertical static force was applied perpendicularly to the implant platform surface, and the external surfaces of the implant body were firmly constrained.

This approach yielded a favourable material distribution for a new implant design, as depicted in Figure 2. Importantly, only the apical part of the implant body volume was subject to removal. Another different topologically optimised design was prepared through the complete elimination of the lower thickness of implant body. Subsequently, an assessment was conducted to compare the fatigue behaviours between the conventional and topologically optimised implants, allowing for an evaluation of their performance.

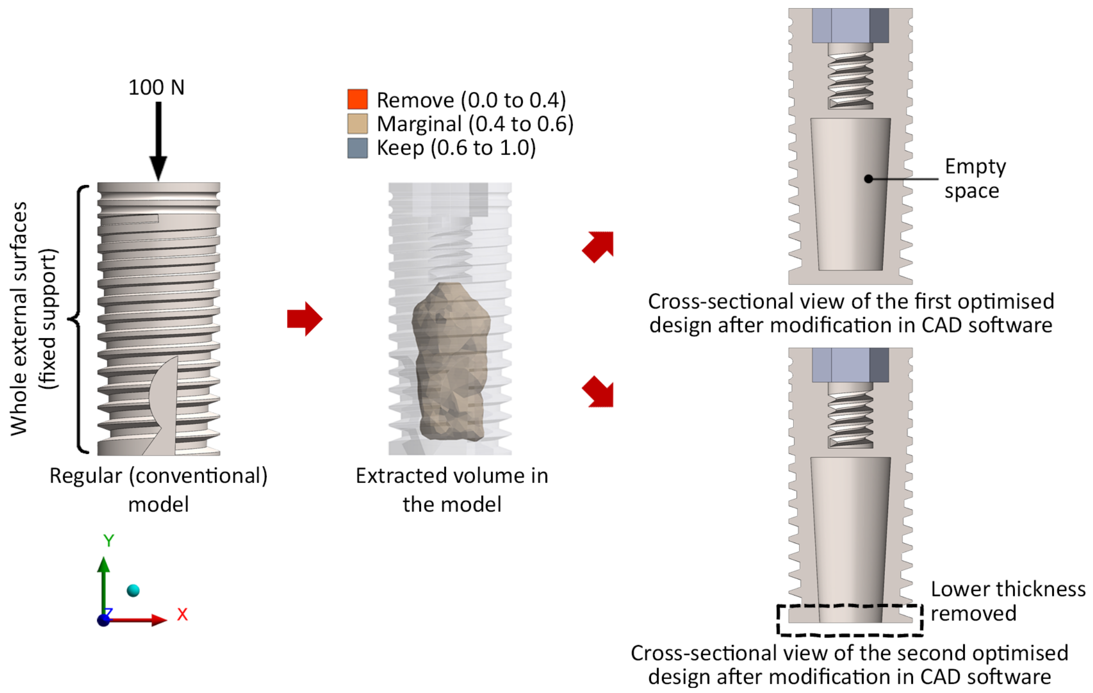

Fig. 2. The key steps taken in the topology optimisation analysis

2.4 Preparation of Meshed Model

Given the intricate and irregular geometrical shapes of the implant components, this study opted for the utilisation of ten-node quadratic tetrahedral elements (SOLID187) to ensure continuousness of force and displacement transmission across nodes. This approach aligns with prior research [28, 29]. It is worth noting that, before the final model discretization, an element sensitivity analysis was conducted to ensure the analysis results remain independent of the mesh conditions. A finer mesh delivers a more accurate solution, yet it comes with the trade-off of increased computational time due to a higher number of nodes and elements. Therefore, a balance must be attained between the optimal element size and the requirement for a dependable solution.

In the assessment of mesh independence, the contact modelling, material properties, loading, and boundary conditions remained consistent with the details outlined in earlier section, including the application of a 100-N load. The analysis involved monitoring the maximum equivalent von Mises stress within the abutment-implant complex across various mesh sizes. A total of nine relative characteristic mesh sizes were examined, ranging from 2.2 mm (Tet A: ~34,000 elements) to 0.7 mm (Tet I: ~865,000 elements).

Once the mesh underwent refinement, the evaluation of the result acceptability hinged on the degree of variation in the critical stress value among the various mesh sizes, with a target threshold of less than 5%. Overall, noticeable variations were observed in the stress magnitudes produced across the range of element sizes. Following four rounds of refinement, the result appeared to stabilize at a mesh size of 1.2 mm (Tet-E), exhibiting a relative deviation of 1.2%. The total number of elements and nodes approximates 176,500 and 250,000, correspondingly. Figure 3 shows both the mesh sensitivity plot and the distribution of the mesh in both the coarse (Tet-A) and refined (Tet-E) models.

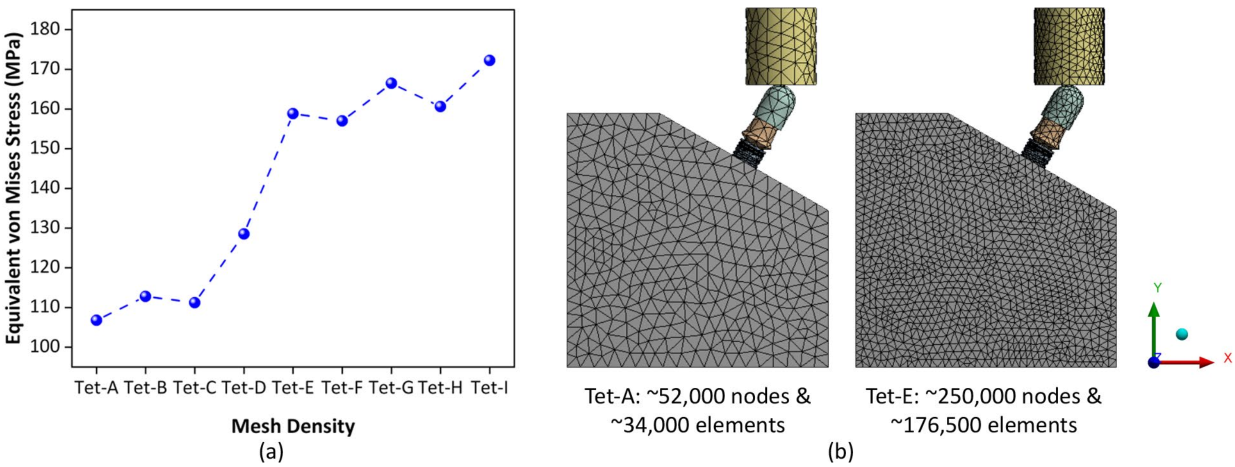

Fig. 3. (a) Mesh sensitivity graph for varying element quantities. (b) The distribution of the mesh in both the less detailed (Tet-A) and the more refined (Tet-E) models

3. Results

3.1 Topology Optimisation Results

The topology optimisation analysis yielded a successful creation of a new implant design. As seen in Figure 2, only the lower third of the implant body underwent alterations, resulting in the removal of its corresponding volume. This adjustment reduced the volume by approximately 24% and 26%, transitioning from 123.13 mm^3 for the traditional implant to 93.63 mm^3 and 91.52 mm^3 for the first and second new designs, respectively. Meanwhile, the reconstruction of the finite element model for the optimised implant assemblies comprised 249,500 nodes and 176,000 elements for the first design, and 249,400 nodes and 175,900 elements for the second design.

3.2 Fatigue Behaviour Results

The study displayed the maximum equivalent alternating stress, minimum fatigue life values and minimum safety factors for all implant designs (regular, optimised design 1, and optimised design 2),

Journal of Advanced Research in Applied Mechanics
Volume 114, Issue 1 (2024) 109-124

considering three different material stiffnesses of the implant body. Additionally, these results were visually represented through a color-coded spectrum scale to facilitate better comprehension.

3.2.1 Maximum equivalent alternating stress results

The traditional implant shape consistently demonstrated a higher maximum equivalent alternating stress magnitude within the implant-abutment assembly compared to the topologically optimised versions, regardless of the material stiffnesses, as indicated in Figure 4(a). As the material stiffness (elastic modulus) increased (from cpTi, Ti-6Al-4V to zirconia), all the three implant designs experienced a linear decrease in stress output, reaching the minimum values of 313.73 MPa for the regular design, 276.31 MPa for the optimised design 1, and 302.96 MPa for the optimised design 2 under zirconia material. Conversely, the highest stress levels were observed under cpTi material, measuring 318.83 MPa, 284.07 MPa, and 306.6 MPa for the regular design, optimised design 1, and optimised design 2, respectively. Notably, the regular design demonstrated approximately 3.4% to 11.9% higher implant stress across all material types when compared to the new designs. A surprising discovery emerged when it was observed that, regardless of material stiffness, topologically optimised design 2 exhibited a higher stress value compared to topologically optimised design 1.

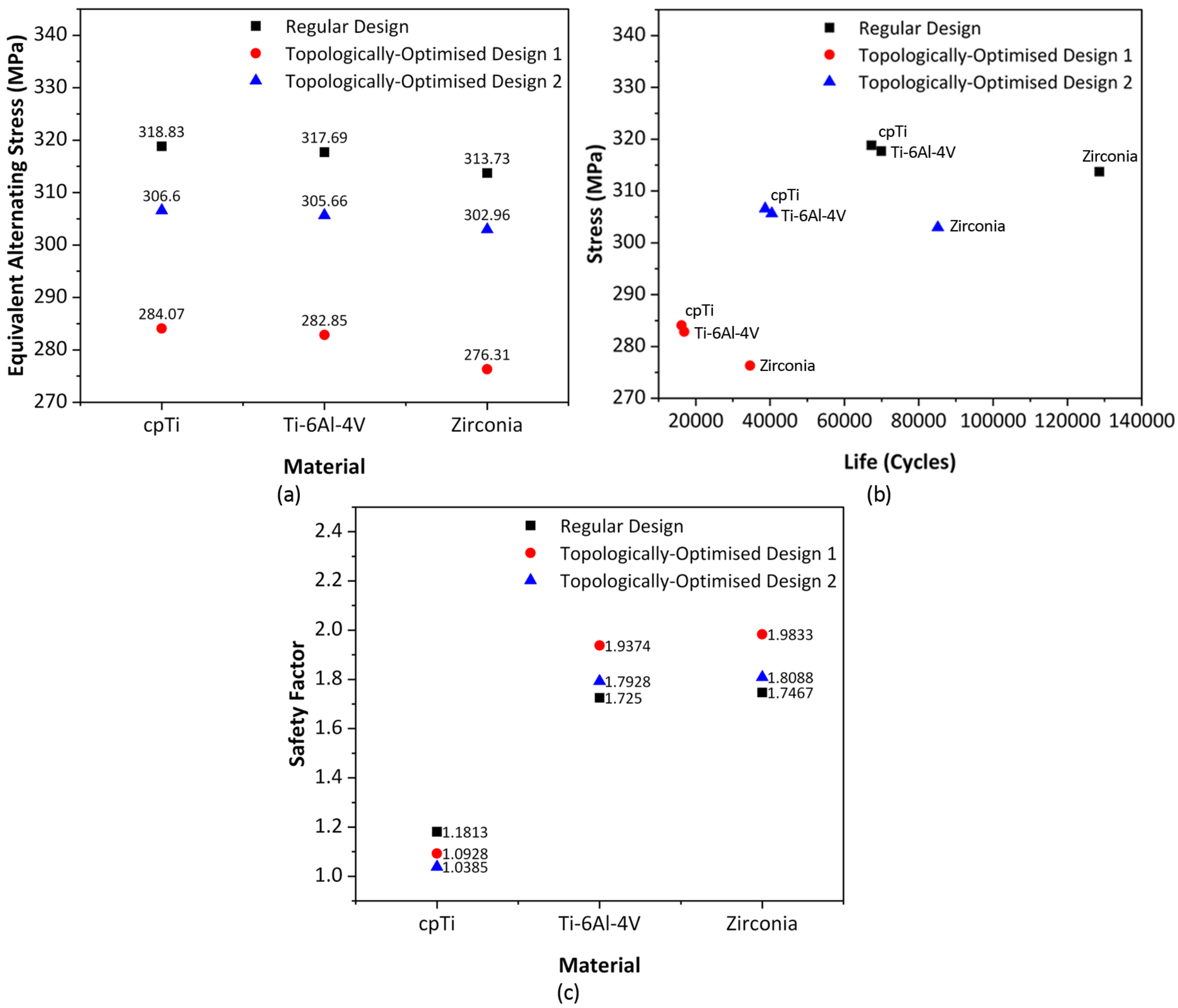

Fig. 4. (a) Maximum equivalent alternating stress, (b) minimum fatigue life, and (c) minimum safety factor of the implant-abutment assembly for all implant designs for each material type

In Figure 5, it is evident that the greatest stress intensity primarily localised in the abutment, particularly at the interfacial surface with the implant platform. Irrespective of the implant designs, an observable region with substantial stress amplification could be seen both around the upper threads of the implant body and near the junction of the holder. The stress concentration area expanded more significantly within the assembly with the increase in the material stiffness value of the implant body, irrespective of the specific implant design. The regular implant design promoted a more adequate stress distribution relative to the optimised ones.

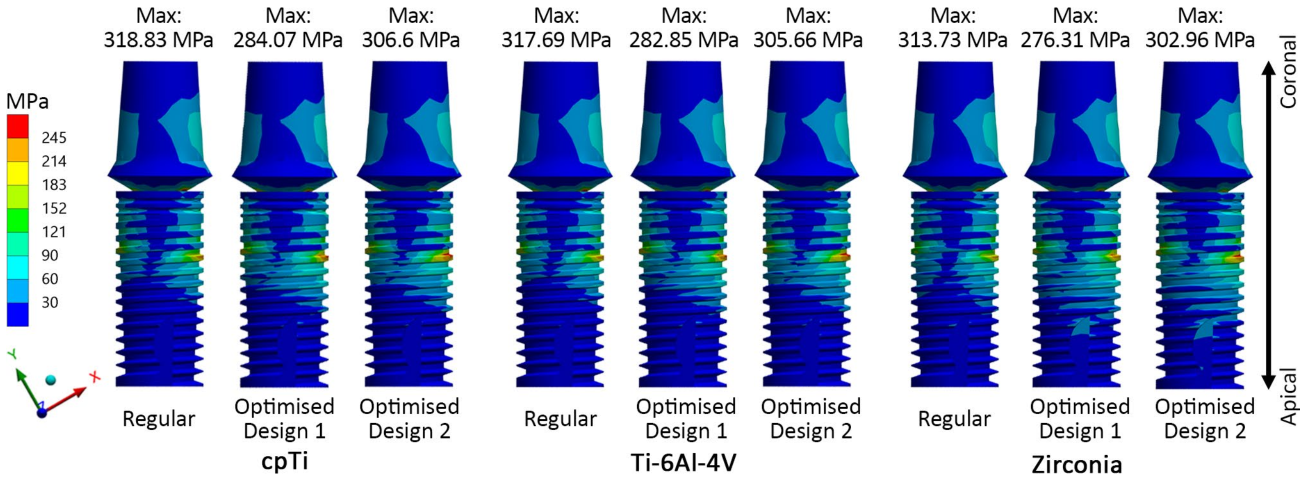

Fig. 5. Dispersion of equivalent alternating stress in the implant-abutment assembly for all implant designs for each material type

3.2.2 Minimum fatigue life results

In Figure 4(b), we can observe a comparison depicting the minimum fatigue life, measured in cycles, for both the traditional and topologically optimised designs. Our findings pointed to the anticipation of fatigue failure only within a specific range of considered material stiffnesses with the applied load of 200 N. This assessment was anchored in the fatigue life limit, set at 5 x 10^6 cycles, derived from prior experimental fatigue testing. The response of the models towards the influence of different material stiffnesses translated to stress levels spanning from 313.73 MPa to 318.83 MPa for the regular implant design, 276.31 MPa to 284.07 MPa for the optimised implant design 1, and 302.96 MPa to 306.6 MPa for the optimised implant design 2. Notably, the regular design generally displayed a longer estimated lifespan, with a maximum cycle number of 1.2861 x 10^5, in contrast to the optimised designs, which exhibited endurance up to 0.34648 x 10^5 (optimised design 1) and 0.85159 x 10^5 cycles (optimised design 2), in all materials. All the maximum cycle numbers were generated by the implant body that made of zirconia. Meanwhile, the lowest cycle numbers for each implant design were attributed to cpTi material that measuring at 0.67285 x 10^5, 0.16233 x 10^5, and 0.38675 x 10^5 cycles for the regular design, optimised design 1, and optimised design 2, respectively.

3.2.3 Minimum safety factor results

Computed in accordance with the Goodman fatigue theory and infinite fatigue life criteria, the safety factor values for fatigue life are represented in Figure 4(c) as a plot of the minimum safety factor within the implant-abutment assembly against material types. The safety factors for the new implant designs had surpassed those of the regular design under Ti-6Al-4V and zirconia materials. In comparison to the conventional model (1.7467), design 1 (1.9833) and design 2 (1.8088), which underwent topological optimisation, displayed 13.5% and 3.5% higher safety factor levels, respectively, for zirconia implant. In contrast, the conventional implant design exhibited a safety factor value higher than that of the optimised designs for cpTi material. The standard model achieved a safety factor value of 1.1813, which is approximately 3 to 5 times higher relative to the optimised designs 1 (1.0928) and 2 (1.0385). It is crucial to highlight that, regardless of the material types used, none of the implant designs displayed a safety factor value below 1.

The colour contour plot highlights that, in all cases, the critical regions at risk of implant failure were consistently identified at the connection region between the abutment and implant, and within the threads close to the midpoint of implant body (Figure 6). The cpTi implants displayed a notably larger area highly susceptible to failure compared to the Ti-6Al-4V and zirconia implants. Besides, topologically optimised design 2 expanded the region vulnerable to failure to a greater extent than the other two designs, irrespective of the material used. Safer regions were predominantly concentrated at the lowermost part of the implant body and the upper section of the abutment in all cases.

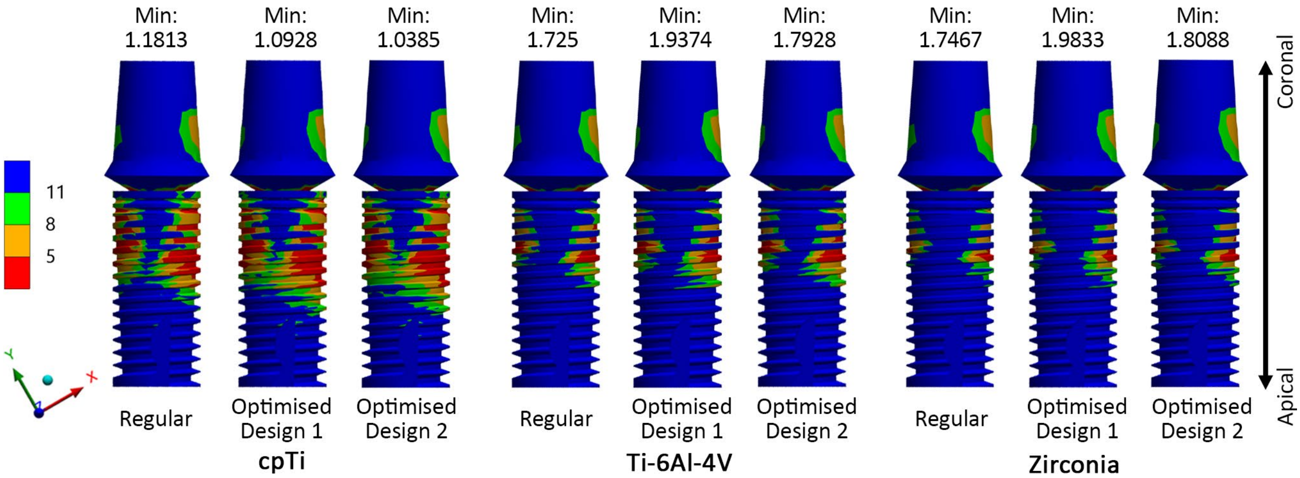

Fig. 6. Distribution of safety factor in the implant-abutment assembly for all implant designs for each material type

4. Discussion

Dental implants serve the vital role of conveying occlusal force to adjacent bones, making the primary design objective centred around enhancing the distribution of external loads to improve implant-supported prosthesis function. Achieving clinical goals necessitates the fusion of fundamental scientific insights concerning geometry and force with innovative engineering solutions. While numerous studies currently explore the endurance of bone-implant attachment to optimize mechanical stimulus transmission, there exists relatively little emphasis and scant information regarding the structural optimization design of dental implants, especially concerning fatigue prediction.

As part of our study on topology optimisation, it was revealed that nearly 24% of the total implant body volume consisted of excessive material (design 1). Design 2, achieved by eliminating the lower structure thickness, results in a volume reduction of approximately 26%. Specifically, the removed material is only from the internal volume of the apical region, leaving other areas untouched. The designated removal areas also encompassed the region beneath the threaded part for securing the abutment screw. However, the volume of that region was not entirely eliminated to ensure the necessary volume for maintaining screw placement and to mitigate the risk of elevated stress generation in that area.

Our findings differ from those of an investigation performed by Chang *et al.,* which reported a lower reduction percentage (approximately 17.9%) in the volume of the traditional implant resulting from topology optimisation [11]. Conversely, Gupta *et al.,* stated a more substantial volume decrease (ranging from 32% to 45%) in their topology study, considering both bone quality and implant microgeometry effects [1]. These variations could potentially be attributed to differences in the structural form of the models and the settings for preliminary processing used in the analysis. Still, the removed material consistently resides in the apical portion of the implant body. For the evaluation of both conventional and topologically optimised implant designs regarding their mechanical and fatigue behaviours, we executed a linear static finite element analysis (FEA), subjecting them to varying material stiffness values in order to analyse mechanical stress, fatigue life, and safety factor of the implant-abutment assembly.

The stress level within the newly modified implants was approximately 3.4% to 11.9% lower than that observed in the regular implant. Interestingly, the way stresses were distributed across various regions within the implant-abutment assembly appeared to be slightly different among the three implant configurations. The findings diverged from those of Chang *et al.,* where the study revealed a 13% increase in implant stress (128.1 MPa) under a 204-N oblique load with the optimised design, as opposed to the original design's stress of 113.3 MPa [11]. In contrast, Gupta *et al.,* [1] results aligned with ours, showing that lower implant stress in the altered design (33.21 MPa) compared to the conventional design (54.26 MPa) at a 50% reduction in volume. One potential explanation for our results is that diminishing the material distribution used for implants generally alleviates the stress shielding phenomenon. Consequently, there is an escalation in the transmission of mechanical stress from the highly rigid implant to the neighbouring bone region characterised by lower stiffness. As a result, the optimised design led to reduced stress on the implant-abutment assembly.

Regarding stress distribution, prominent stress intensification was observed around the area of abutment connection and implant threads close to the junction of the holder, aligning with the stress distribution patterns depicted in prior research [1, 11]. The high stress concentration observed at the middle threads of the implant body and its surrounding area may result from the resistance imposed by the holder as it bears the load applied on the implant body. It can be inferred that volume reduction from the implant's end to its mid-region is feasible. Shi *et al.,* found that a larger, gradually tapering crestal part radius was the favoured choice for an alternative implant design due to lower peak stress generation compared to commercially available implants [10]. Additionally, by offering additional spaces in the apical part, the topologically optimised implant design has a higher potential to improve osseointegration ingrowth [30].

Relating the stress results to more realistic scenarios involving biological factors, it is commonly observed that the interface of implant with the compact or peri-implant bone experiences a high stress intensity. Exceeding the strength of cortical bone at 170 MPa, bone stress is foreseen to result in bone failure. In dental implantology, marginal bone resorption is a significant concern, potentially resulting in patient complaints, aesthetic issues, soft and hard tissue deformations, and even implant extraction [31]. The initial year following implantation frequently reveals a more pronounced reduction in bone level, averaging about 1.0 mm, but subsequently decreasing to 0.2 mm in the next years. The occurrence of implant failure may be attributed to implant loosening and fractures caused by the resorption of supporting bone. Therefore, minimising the impact of bone loss is crucial, and achieving optimal transfer of mechanical forces at the bone-implant interface is essential.

In the present study, the implant body was analysed in three different prevalent implant material options which are cpTi, Ti-6Al-4V, and zirconia. Regardless of the implant designs and material stiffnesses (ranging from 276.31 to 318.83 MPa), we found that the peak implant stress remained below the yield strength of each corresponding material type investigated; cpTi (480 MPa), Ti-6Al-4V (847 MPa) [19], and zirconia (2000 MPa). This suggests a high likelihood of implant success and a low risk of failure.

In evaluating fatigue behaviour, a single cycle of loading used in the analysis involved a 30° tilted load [26]. All the three implant configurations endured different maximum fatigue life which are up to 1.2861 x 10^5 cycles for the regular design, 0.34648 x 10^5 cycles for the optimised design 1, and 0.85159 x 10^5 cycles for the optimised design 2, under zirconia material. However, when the implant body was assigned with the lowest material stiffness (cpTi), all the implant designs experienced a shorter estimated lifetime with the regular, optimised design 1, and optimised design 2 yielded 0.67285 x 10^5, 0.16233 x 10^5, and 0.38675 x 10^5 cycles, respectively. These results align with ISO 14801 standards, which specify that dental implants should withstand a minimum of 5 x 10^6 cycles without exhibiting damage [21]. Consequently, the conventional implant design is anticipated to exhibit greater resistance to fatigue failure over its lifespan compared to the optimised designs. But if the topologically optimised shape is of concern, design 2 is more favourable as it had offered improved life cycles than design 1.

All safety factors for the implant-abutment assembly were exceeded 1 for all implant designs and material types. With the increased stress levels in the implant assembly, the safety factor values decreased accordingly, with the lowest value recorded by the cpTi implant, regardless of the implant geometries. Of the implant designs, the topologically optimised design 1 led to the highest score of safety factor in both Ti-6Al-4V and zirconia materials, followed by the optimised design 2 and regular ones. However, the regular implant being the most stable structure for cpTi material in comparison to others. Thus, from a mechanical perspective, the topologically optimised implants seem to offer acceptable and adequate structural stability for dental implant applications. In all scenarios, it was consistently observed that the middle threads and their surrounding region exhibited a higher susceptibility to failure. This susceptibility may be attributed to the concentration of excessive stress in these areas, primarily due to the absence of supporting structures to counteract the bending effect induced by the applied load. It is anticipated that the zone prone to failure would broaden with an increased reduction in bone level and, conversely, narrow with a lesser reduction, offering insights into the predictive nature of this phenomenon.

Despite the robustness of the findings, it is essential to acknowledge that the quantitative data obtained are predictive and subject to several limitations in the analyses. Specifically, the implant was tested within non-living materials under static loading conditions, whereas real-life applications involve placement within complex living tissues with unpredictable patterns, potentially influencing the results. Furthermore, our investigation solely focused on a single type of restoration, and therefore, the findings pertain exclusively to this specific treatment modality.

Future studies in implant dentistry including topology optimisation can explore various aspects, including the assessment of different implant body dimensions and physiological loading conditions, the incorporation of realistic dynamic occlusal loading, the utilisation of more intricate geometric models, and the simulation of implant removal from bone hole. While our current findings may not be directly applicable to clinical scenarios, they do provide valuable insights into mechanical and fatigue responses through computational analysis. Ultimately, further *in vitro* and *in vivo* investigations are warranted to validate implant durability under real-world conditions, especially at lower levels of stress. As for our study's null hypothesis, it was rejected due to the observed significant differences between traditional and topologically optimised implant designs in their respective responses.

5. Conclusion

Through the parametric analyses performed in this study, the following conclusions are drawn. The newly designed implants achieved a remarkable 24% and 26% reduction in volume compared to the traditional implant. Importantly, these topologically optimised designs generally preserved implant stability under various implant material stiffnesses. The topologically optimised implant designs demonstrated a reduction in equivalent alternating stress by nearly 3.4% to 11.9% compared to the regular implant. Nevertheless, the regular implant design resulted in a longer fatigue life of approximately 33.8% to 75.9% than the optimised implant designs. Regarding safety factors, the implants subjected to topology optimisation generally exhibited safety factor levels about 3.5% to 13.5% higher than those of the regular design. Of all materials investigated, the implant with a higher stiffness (elastic modulus) is observed to be favourable as it produced a lower implant stress, higher fatigue life, and higher safety factor than the less stiff implant irrespective of the implant designs.

Acknowledgement

The authors would like to acknowledge the support from Fundamental Research Grant Scheme (FRGS) under a grant number of FRGS/1/2020/TK0/UNIMAP/03/2 from the Ministry of Higher Education Malaysia. The authors reported no conflicts of interest related to this study.

References

[1] Gupta, Yash, Iyer, Rohit, Dommeti, Vamsi Krishna, Nutu, Emil, Rana, Masud, Merdji, Ali, Biswas, Jayanta Kumar, and Roy, Sandipan. "Design of dental implant using design of experiment and topology optimization: A finite element analysis study." *Proceedings of the Institution of Mechanical Engineers, Part H: Journal of Engineering in Medicine* 235, no. 2 (2020): 157-166. https://doi.org/10.1177/0954411920967146

[2] Tomasi, Cristiano and Derks, Jan. "Etiology, occurrence, and consequences of implant loss." *Periodontology 2000* 88, no. 1 (2022): 13-35. https://doi.org/10.1111/prd.12408

[3] Agustin-Panadero, R., Leon-Martinez, R., Labaig-Rueda, C., Faus-Lopez, J., and Sola-Ruiz, M. F. "Influence of implant-prosthetic connection on peri-implant bone loss: A prospective clinical trial with 2-year follow-up." *The International Journal of Oral & Maxillofacial Implants* 34, no. 4 (2019): 963-968. https://doi.org/10.11607/jomi.7168

[4] Thanissorn, Charn, Guo, Jason, Jing Ying Chan, Dianna, Koyi, Bryar, Kujan, Omar, Khzam, Nabil, and Miranda, Leticia A. "Success rates and complications associated with single immediate implants: A systematic review." *Dentistry Journal* 10, no. 2 (2022). https://doi.org/10.3390/dj10020031

[5] Samieirad, Sahand, Mianbandi, Vajiheh, Shiezadeh, Farid, Hosseini-Abrishami, Majid, and Tohidi, Elahe. "Tapered versus cylindrical implant: Which shape inflicts less pain after dental implant surgery? A clinical trial." *Journal of Oral and Maxillofacial Surgery* 77, no. 7 (2019): 1381-1388. https://doi.org/10.1016/j.joms.2019.02.027

[6] Bidez, M. W., and C. E. Misch. "Chapter 5–Clinical Biomechanics in Implant Dentistry." *Dental Implant Prosthetics* (2015): 95-106. https://doi.org/10.1016/B978-0-323-07845-0.00005-1

[7] Ishak, Muhammad Ikman, Daud, Ruslizam, and Mohd Noor, Siti Noor Fazliah. "The effect of material stiffness on dental implant stability – A finite element analysis." *ASEAN Engineering Journal* 13, no. 1 (2023): 59-67. https://doi.org/10.11113/aej.v13.18087

[8] Gil, Javier, Sandino, Clara, Cerrolaza, Miguel, Pérez, Román, Herrero-Climent, Mariano, Rios-Carrasco, Blanca, Rios-Santos, Jose V., and Brizuela, Aritza. "Influence of bone-level dental implants placement and of cortical thickness on osseointegration: In silico and in vivo analyses." *Journal of Clinical Medicine* 11, no. 4 (2022): https://doi.org/10.3390/jcm11041027

[9] Chang, C. L., Chen, C. S., and Hsu, M. L. "Biomechanical effect of platform switching in implant dentistry: A three-dimensional finite element analysis." *The International Journal of Oral & Maxillofacial Implants* 25, no. 2 (2010): 295-304.

[10] Shi, L., Li, H., Fok, A. S., Ucer, C., Devlin, H., and Horner, K. "Shape optimization of dental implants." *The International Journal of Oral & Maxillofacial Implants* 22, no. 6 (2007): 911-20.

[11] Chang, Chih-Ling, Chen, Chen-Sheng, Huang, Chang-Hung, and Hsu, Ming-Lun. "Finite element analysis of the dental implant using a topology optimization method." *Medical Engineering & Physics* 34, no. 7 (2012): 999-1008. https://doi.org/10.1016/j.medengphy.2012.06.004

[12] Seitz, K. F., Grabe, J., and Köhne, T. "A three-dimensional topology optimization model for tooth-root morphology." *Computer Methods in Biomechanics and Biomedical Engineering* 21, no. 2 (2018): 177-185. https://doi.org/10.1080/10255842.2018.1431778
[13] Zhong, Zheng-Cheng, Wei, Shun-Hwa, Wang, Jung-Pin, Feng, Chi-Kuang, Chen, Chen-Sheng, and Yu, Chung-huang. "Finite element analysis of the lumbar spine with a new cage using a topology optimization method." *Medical Engineering & Physics* 28, no. 1 (2006): 90-98. https://doi.org/10.1016/j.medengphy.2005.03.007
[14] Nayak, Chitresh, Singh, Amit, and Chaudhary, Himanshu. "Topology optimisation of transtibial prosthesis socket using finite element analysis." *International Journal of Biomedical Engineering and Technology* 24, no. 4 (2017): 323-337. https://doi.org/10.1504/IJBET.2017.085438
[15] Khan, Mohammed Irfan, and Chitresh Nayak. "Topology optimization of mono leaf spring for electric vehicle using finite element analysis." *International Journal on Interactive Design and Manufacturing (IJIDeM)* (2022): 1-8. https://doi.org/10.1007/s12008-022-01073-y
[16] Zhang, Kaiqing, Cheng, Gengdong, and Xu, Liang. "Topology optimization considering overhang constraint in additive manufacturing." *Computers & Structures* 212 (2019): 86-100. https://doi.org/10.1016/j.compstruc.2018.10.011
[17] Islam, Md Saifi Bin, Ahmed, Muhammad Faiz, and Abdullah Al, Saad. "Numerical investigation on the aerodynamic characteristics of a wing for various flow and geometrical parameters." *Malaysian Journal on Composites Science and Manufacturing* 12, no. 1 (2023): 13-30. https://doi.org/10.37934/mjcsm.12.1.1330
[18] Quanjin, Ma, Merzuki, M. N. M., Rejab, M. R. M., Sani, M. S. M., and Bo, Zhang. "Numerical investigation on free vibration analysis of kevlar/glass/epoxy resin hybrid composite laminates." *Malaysian Journal on Composites Science and Manufacturing* 9, no. 1 (2022): 11-21. https://doi.org/10.37934/mjcsm.9.1.1121
[19] Lee, Hyeonjong, Jo, Minhye, and Noh, Gunwoo. "Biomechanical effects of dental implant diameter, connection type, and bone density on microgap formation and fatigue failure: A finite element analysis." *Computer Methods and Programs in Biomedicine* 200 (2021): 105863. https://doi.org/10.1016/j.cmpb.2020.105863
[20] Yao, Kuang-Ta, Chen, Chen-Sheng, Cheng, Cheng-Kung, Fang, Hsu-Wei, Huang, Chang-Hung, Kao, Hung-Chan, and Hsu, Ming-Lun. "Optimization of the conical angle design in conical implant–abutment connections: A pilot study based on the finite element method." *Journal of Oral Implantology* 44, no. 1 (2018): 26-35. https://doi.org/10.1563/aaid-joi-D-17-00149
[21] Bayata, Fatma and Yildiz, Cengiz. "The effects of design parameters on mechanical failure of Ti-6Al-4V implants using finite element analysis." *Engineering Failure Analysis* 110 (2020): 104445. https://doi.org/10.1016/j.engfailanal.2020.104445
[22] Yalçın, Mustafa, Kaya, Beyza, Laçin, Nihat, and Arı, Emre. "Three-dimensional finite element analysis of the effect of endosteal implants with different macro designs on stress distribution in different bone qualities." *The International Journal of Oral & Maxillofacial Implants* 34, no. 3 (2019): e43–e50. https://doi.org/10.11607/jomi.7058
[23] Brune, Annike, Stiesch, Meike, Eisenburger, Michael, and Greuling, Andreas. "The effect of different occlusal contact situations on peri-implant bone stress – A contact finite element analysis of indirect axial loading." *Materials Science Engineering: C* 99 (2019): 367-373. https://doi.org/10.1016/j.msec.2019.01.104
[24] Tretto, Pedro Henrique Wentz, dos Santos, Mateus Bertolini Fernandes, Spazzin, Aloisio Oro, Pereira, Gabriel Kalil Rocha, and Bacchi, Atais. "Assessment of stress/strain in dental implants and abutments of alternative materials compared to conventional titanium alloy - 3D non-linear finite element analysis." *Computer Methods in Biomechanics and Biomedical Engineering* 23, no. 8 (2020): 372-383. https://doi.org/10.1080/10255842.2020.1731481
[25] Wang, Kun, Geng, Jianping, Jones, David, and Xu, Wei. "Comparison of the fracture resistance of dental implants with different abutment taper angles." *Materials Science and Engineering: C* 63 (2016): 164-171. https://doi.org/10.1016/j.msec.2016.02.015
[26] Zhang, Xuetao, Mao, Jian, Zhou, Yufeng, Ji, Fangqiu, and Chen, Xianshuai. "Study on statics and fatigue analysis of dental implants in the descending process of alveolar bone level." *The Proceedings of the Institution of Mechanical Engineers Part H* (2020): 0954411920926080. https://doi.org/10.1177/0954411920926080
[27] Jeng, Ming-Dih, Lin, Yang-Sung, and Lin, Chun-Li. "Biomechanical evaluation of the effects of implant neck wall thickness and abutment screw size: A 3D nonlinear finite element analysis." *Applied Sciences* 10, no. 10 (2020): https://doi.org/10.3390/app10103471
[28] Amruta, Gujar, Rajeev, Singh, Gaurang, Mistry, Simran, Moorjani, Mishal, D”souza, and Kunal, Mehta. "Comparative evaluation of stress on the peri-implant bone of different densities in mandible restored by various diameter of implants - A finite element analysis." *Journal of Electronics Information Technology Science And Management* 12, no. 11 (2022): 161-177.

[29] Satheesh Kumar, P., Satheesh, K. K., John, J., Patil, G., and Patel, R. "Force transfer and stress distribution in an implant-supported overdenture retained with a hader bar attachment: A finite element analysis." *ISRN Dent* 2013 (2013): 369147. https://doi.org/10.1155/2013/369147

[30] Lawrence, Abner Ankit, Singh, Nikhil, Davis, Rahul, Sahil Ansari, Mohd, Tewari, Yash Vardhan, and Francis, Vishal (2022). *Topological Design Optimisation of Dental Implant*. Optimization of Industrial Systems. https://doi.org/10.1002/9781119755074.ch13

[31] Naveau, Adrien, Shinmyouzu, Kouhei, Moore, Colman, Avivi-Arber, Limor, Jokerst, Jesse, and Koka, Sreenivas. "Etiology and measurement of peri-implant crestal bone loss (CBL)." *Journal of Clinical Medicine* 8, no. 2 (2019): https://doi.org/10.3390/jcm8020166